Available online at www.sciencedirect.com
SCIENCE DIRECT
Polymer 46 (2005) 10989–10995
polymer
www.elsevier.com/locate/polymer

Stress softening experiments in silica-filled polydimethylsiloxane provide insight into a mechanism for the Mullins effect

David E. Hanson[a,*], Marilyn Hawley[b], Robert Houlton[b], Kiran Chitanvis[b], Philip Rae[b], E. Bruce Orler[b], Debra A. Wrobleski[b]

[a] *Theoretical Division, Los Alamos National Laboratory, MS B268, Los Alamos, NM 87544, USA*
[b] *Materials Science and Technology Division, Los Alamos National Laboratory, Los Alamos, NM 87545, USA*

Received 14 July 2005; received in revised form 6 September 2005; accepted 7 September 2005
Available online 30 September 2005

Abstract

Under repeated tensile strain, many particle-filled polymers such as silica-filled polydimethylsiloxane (PDMS), exhibit a reduction in stress after the initial extension, the so-called Mullins effect, and the mechanism(s) responsible for this is considered to be a major unsolved mystery of polymer physics. We report here the first observation of the absence of this effect in cross linked, silica-filled PDMS when the second strain axis is perpendicular to the initial strain axis. This result poses a challenge for existing theories. We propose a mechanism to account for the Mullins effect that is consistent with our experimental observations.

Keywords: Polydimethylsiloxane; Mullins effect; Stress softening

1. Introduction

Filled polymers, such as silica-filled polydimethylsiloxane (PDMS) and carbon black filled rubbers, are an important class of materials with applications ranging from sealants to the familiar automobile tire tread compound. Under tensile strain, they invariably exhibit a reduction in stress on the second and subsequent extensions, a phenomenon that has come to be known as the Mullins effect [1,2]. While the term has been applied to unfilled rubbers and even biological systems [3], its first association was with filled polymers. Although stress softening does occur in unfilled rubbers, its behavior is fundamentally different [4] from what is observed in filled polymers. As the material is sequentially taken through multiple extension/retraction strain cycles to higher strains, the stress does not asymptote to the stress observed for a single extension of virgin material as is observed for filled systems. Moreover, the temperature dependence of the stress during the initial extension of silica-filled PDMS is opposite that for subsequent extensions. Initially, it displays a negative correlation with temperature [5], while subsequent extensions usually show a positive correlation. The initial tensile stress observed in unfilled rubbers invariably correlates positively with temperature. It is likely that the fundamental mechanisms governing stress softening are very different for filled and unfilled polymers. Understanding the underlying physical mechanism is considered crucial to the development of predictive constitutive and aging models for these materials. However, despite more than 50 years of research, the origin of the Mullins effect is still considered 'one of the most important problems in rubber elasticity' [6]. The phenomenon was first reported in 1938 by Holt [7], but appears in an even earlier work by Gurney and Tavener [8] dealing with energy loss in carbon-black-filled rubber. In 1944, Alexandrov and Lazurhin [9] proposed a mechanism based on polymer chains slipping across the surface of the carbon black filler to account for the stress reduction. Mullins and Tobin [10] performed more systematic studies of the phenomenon in 1957 and postulated a mechanism for its cause. They proposed a phenomenological model in which the filled polymer was assumed to exist in two phases (or zones), one soft having a lower modulus, the other hard, with a high modulus. The tensile stress was assumed to be a linear combination by volume fraction. Under strain, they postulated that hard phase regions were converted to soft ones, reducing the stress. Later, Mullins developed an elasticity model [2] containing a damage parameter that he was able to fit

* Corresponding author. Tel.: +1 505 667 2306; fax: +1 505 665 3909.
E-mail addresses: deh@lanl.gov (D.E. Hanson), hawley@lanl.gov (M. Hawley), houlton@lanl.gov (R. Houlton), kiranc@lanl.gov (K. Chitanvis), prae@lanl.gov (P. Rae), eborler@lanl.gov (E.B. Orler), wrobleski@lanl.gov (D.A. Wrobleski).

0032-3861/$ - see front matter © 2005 Published by Elsevier Ltd.
doi:10.1016/j.polymer.2005.09.039

to their tensile stress/strain experiments. Interestingly, Mullins did report [11] observing anisotropy in the stress softening in carbon black filled rubber under tensile strain, but he did not speculate on a mechanism to explain it nor attempt to incorporate this phenomenon in his models. Bueche [12] proposed the idea that chains connecting adjacent filler particles were comprised of a distribution of lengths. He argued that stress softening was due to the shorter chains becoming taut and tearing loose from the filler particles under strain. He also developed a mathematical formalism based on classical elasticity theory to describe the change in stress between the first and subsequent extensions.

The focus of current theoretical work on the Mullins effect [13–19] is predominately the modification of conventional elasticity theories to include a phenomenological damage parameter to describe the stress softening. The material behavior is complex and, not surprisingly, theoretical models have generated controversy [20,21]. With parameter values determined by fits to experiment, the models provide useful constitutive relations that can be incorporated into large finite-element engineering codes. However, the theories are purely phenomenological, containing no underlying physical structure or mechanisms. The mathematical formalism typically ignores stress hysteresis and permanent set (the incomplete recovery of strained material to its original shape), and since the theories are based on either traditional multi-chain molecular network theories or continuum mechanics, they are inherently isotropic. As such, none are consistent with our experimental observations, reported below. Perhaps, the most interesting recent paper for our present work is due to Horgan et al. [22] in which they present a stress softening theory based on a modified Gent model of rubber elasticity [23]. They conclude that the phenomenon of stress softening under tensile strain is clearly anisotropic. Lacking relevant experimental data, a specific anisotropic model was not presented.

2. Material preparation

The PDMS fumed silica composite material was prepared using dimethyl methylvinyl siloxane copolymer (weight averaged molecular weight ~300,000 Da), purchased from United Chemical Technologies, Inc. Petrarch® (PS255), with 0.113% methylvinyl groups. The repeat, or backbone unit of PDMS is composed of a silicon atom bound to two methyl groups and an oxygen atom, $-[(CH_3)_2Si-O]-$. Filler material, amorphous silicon dioxide (SID 3352), having a specific area of 200 m^2/g, and a curing agent, 2,4-dichlorobenzoyl peroxide 50% in PDMS (SIS 6960), were purchased from Gelest, Inc. All materials were used as received. The composite material was prepared by weighing out the PS255 gum in a plastic mixing jar in SpeedMixer™ DAC 150 FV, dual axial mixer. The silicon dioxide filler (35 parts per hundred relative to the PDMS) was added, followed by mixing at 3500 rpm for 45 s and cooled in an ice bath. This procedure was repeated until addition of the filler was complete. After the addition of the filler, the peroxide curing agent was added, and the mixture was placed between Teflon sheets and pressed into a thin sheet, approximately 150 mm in diameter and 1 mm thick. The pressing conditions were: 6000 psi at 115 °C in a Carver hydraulic press equipped with heated platens and a constant pressure controller. The sample was heated for 4 h then cooled to room temperature overnight at 6000 psi. The sheets were then placed in a 150 °C oven for 4 h, then cooled to room temperature.

3. Experimental discussion

Large dog-bone shaped samples, approximately 110 mm long by 25 mm wide, were diecut from the material prepared as described above. Tensile prestraining of active lengths of about 50 mm to between 150 and 200% were carried out on an Instron 1125 load-frame with MTS Testworks 4.0 software at a cross-head speed was 50 mm/min. Owing to the deformation of the gripping lugs, there was some slippage and the effective extension rate was only about 25 mm/min, corresponding to a nominal strain rate of $\sim 0.008\ s^{-1}$. The slippage also introduced some uncertainty into the actual value of the prestrain. Smaller dog-bone samples (10 mm long, 2 mm wide, and nominally 1 mm thick) were die-cut from the prestrained material and subjected to strains of up to 300% at a strain rate of $\sim 0.01\ s^{-1}$ using a small Fullam tensile stage designed to fit in a Veeco Metrology atomic force microscope. Control samples that were not prestrained, were die-cut from the same stock as the large dog bones and tested in the same way. Stress and strain were recorded at strain increments of ~0.03%. In this paper, all references to stress will be the 'engineering' stress, i.e. the tensile force divided by the original, unstrained cross sectional area.

Fig. 1 shows the stress/strain behavior of a control sample of silica-filled PDMS through sequential extension/retraction cycles, up to maximum strains of 100, 200 and 300%. Any permanent set that occurred during each cycle, typically in the range of 3–6% of the original length [24], has been removed by re-registering the zero stress/strain point to

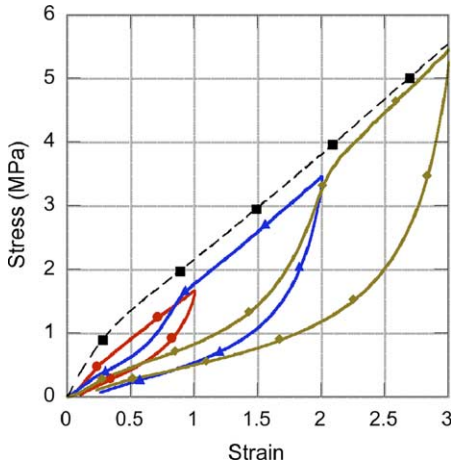

Fig. 1. Sequential tensile strain cycles for virgin silica-filled PDMS sample showing stress softening: first pull to 100% (circles), second pull to 200% (triangles), third pull to 300% (diamonds). Also shown is the initial stress/strain for a separate sample pulled to 300% (squares).

the origin. The stress was not corrected for the slight change in thickness caused by the permanent set. Several features are apparent. Most important, we see that the stress is reduced on subsequent extensions up to the maximum previous strain, the Mullins effect. Also, shown for comparison is the stress for an independent sample, strained to 300%. For each cycle, we note that for strains above the previous maximum, the stress rejoins the curve that would be observed for a continuous first extension; the material appears to remember how far it was previously strained. The difference between the asymptotic strain for the cycled sample and the continuous extension to 300% is due to inherent sample-to-sample variations. Although not shown in this figure, we have observed that, after the second strain, very little additional softening occurs up to the same maximum. We also see a pronounced hysteresis in the stress within each strain cycle; the stress during the retraction phase is always much less than that during extension. The stress softening produced during the initial extension of silica-filled PDMS is also permanent; second extensions taken up to 26 weeks after the first, show no significant stress recovery [24].

Motivated by the arguments for a stress softening mechanism given below, we prestrained a large dog-bone to 170% and then die-cut smaller dog-bones from the center region, two each parallel and perpendicular to the original prestrain axis. Both sets were subjected to a second tensile strain. One of each set was cycled sequentially to maximum strains of 100, 200 and 300%, while the second in each set was given a single extension to 300%. As shown in Fig. 2, the stress/strain behavior of the latter perpendicular sample shows no evidence of stress softening, establishing that the Mullins effect is not present if the second strain axis is perpendicular to the first. For comparison, we also show the stress/strain curve for the secondary strain of the small parallel dog-bone where the Mullins effect is clearly present. The data for the cyclic stress/strain test for the second perpendicular dog-bone sample

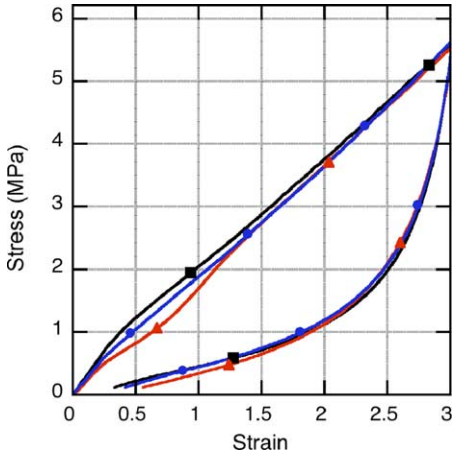

Fig. 2. Tensile stress/strain for secondary strain for small dog-bone samples cut and strained perpendicular to initial strain axis (circles), and parallel (triangles). Also shown for comparison is initial stress/strain for a control sample (squares). Note that stress softening is not apparent in the secondary stress curve strained perpendicular to the original strain axis.

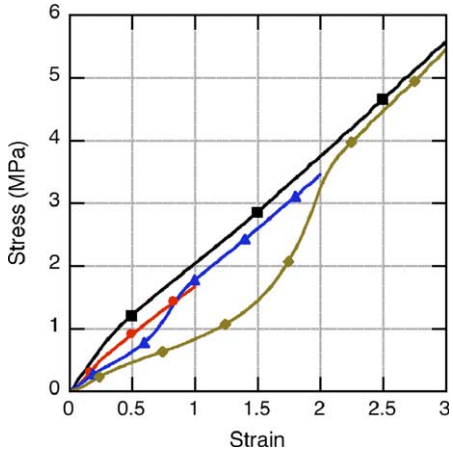

Fig. 3. Secondary cyclic tensile stress/strain data for a small dog-bone cut perpendicular to first strain axis, elongated sequentially to 100%, (circles) 200% (triangles), then 300% (diamonds). Also shown for comparison is the initial stress/strain for a control sample (squares).

is shown in Fig. 3 and compared to a control sample. In both Figs. 2 and 3 and the cyclic data for the second parallel sample (data not shown) a clear Mullins effect is only present when the sample is strained parallel to the first strain axis. Note also the similarity in shape between the data in Fig. 1 for the sample that was not prestrained and that for the sample in Fig. 3 where the secondary strain was perpendicular to the original strain axis. We attempted to extend this procedure to tertiary strains, by cutting an even smaller sample from the twice-strained sample, perpendicular to the second strain axis (parallel to the first strain axis) to determine whether the Mullins effect could be removed again. Unfortunately, this sample was too small to mount in our tensile stage.

We also cut samples at angles of 15, 20, 30, 45, and 60° from two other prestrained large dog-bones. Although the results were inconclusive, generally, the low angle samples appeared to exhibit a Mullins effect somewhat reduced from that of the 0° (parallel) sample while the data for the higher angle samples showed little or no Mullins effect. Direct comparison between the data for the two sets of samples was complicated by the fact that the low and high angle samples were cut from different prestrained large dog-bones, which had been strained different amounts.

4. Proposed mechanism for stress softening

Like other investigators [5,12,13,15,25,26] we envision silica-filled PDMS to be a continuous, high functionality network of polymer chains connected to silica filler particles by Van der Waals' and electrostatic forces. Although these interactions are commonly referred to as non-bonded interactions, for convenience, we shall use the term 'bonds' when referring to them. When exposed to ambient air, the fumed-silica particles interact with water forming hydroxyl groups on the surface. Simulations [27] suggest that the PDMS molecules can interact with these hydroxyl groups. It is also observed experimentally [28] that chemically treating the silica particles

to remove these hydroxyl sites can cause a large decrease in tensile stress/strain curve. It is this interaction that is thought to give rise to an adhesive force between the PDMS chains and the silica particles. Since the Mullins effect is commonly observed only in filled polymer systems, we shall focus on polymer/filler particle interactions and ignore network chain crosslinks in this discussion. Crosslinks are covalent chemical bonds that are much stronger than the non-bonded interactions between the chains and filler particles, their principal effect being to reduce the effective chain length between filler particle nodes. Our previous work [29] suggests that the amount of PDMS chain that is bound to the surface is on the order of 6 backbone sites on the polymer, with an average total binding energy of about 25 kcal/mol. Fig. 4 shows a schematic of two network chains, each connected to two silica filler particles that serve as network nodes. Although we have depicted the particles as spheres, atomic force microscope images [24,30] clearly show that they are actually non-uniformly dispersed aggregates containing on the order of tens of smaller, nearly perfect $\sim$10 nm spheres of silica. We have chosen a representative configuration, in which one chain (connecting nodes C and D) is oriented in the plane of the figure, and the other chain (connecting nodes A and B) passes under chain CD and is oriented close to normal to the page. Nodes C and D are closer together than A and B and the chain connecting them has more slack than chain AB. We shall use the term 'entanglement' to refer to the chain conformations and the alignment of their end-to-end vectors relative to the strain axis. As the network undergoes tensile strain in the direction shown by the arrow, at some value of strain, chain AB becomes taut before chain CD and, due to the entanglement constraint provided by chain CD and particle D, it arrives at the surface of node D at the point where chain CD is attached. As the strain is incrementally increased to some value σ, chain AB must pass between chain CD and its attachment points on particle D, in effect, removing the entanglement. We shall refer to this event as a 'chain-crossing'. It can do this by displacing the bonded portion of the chain, a few backbone units at a time, perhaps only one. The exposed bonding sites can temporarily bond to chain AB as it slides across the surface, giving rise to a frictional force. It is unlikely that the chain AB could slip at either of its attachment points on particles A or B because that would involve the simultaneous displacement of all of its bonding sites as opposed to one or a few sites on chain CD. After chain AB passes under a backbone unit of CD, the displaced region of chain CD can rapidly reattach allowing it to remain continuously bound to particle D. Once chain AB has completely traversed the attachment region on particle D, the original entanglement is permanently removed. When the tensile stress is reduced, the material will relax to nearly its original length due to retractive forces arising in the extended chains. Any chain crossings that have been removed in this manner will not be re-established because of two conditions: no constraints exist to force the chains to slide between a bound chain and the particle to which it is attached. Secondly, stress hysteresis (Fig. 1) clearly shows that the retractive force is much weaker than that of extension. Consequently, the next time the material is strained along the same axis up to σ, previously removed entanglements will not be present and the amount work required will perforce be reduced.

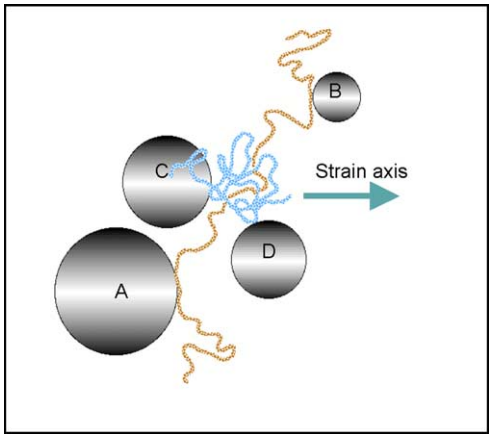

Fig. 4. Schematic of polymer chain and filler particle node network showing two 'entangled' chains.

We propose that it is this removal of entanglements that causes the stress to be lower on the second and subsequent strains, i.e. provides the mechanism for stress softening. This mechanism differs significantly from previous theories. Unlike Mullins' early proposal requiring that the material exist in two 'zones', having high and low elastic moduli, our mechanism requires only a single elastic medium. It is also fundamentally different from models that assume that the material undergoes permanent 'damage' as chains are torn loose from the surface of filler particles. This would imply that stress softening occurs because the number of network chains is reduced, but this is not compatible with our observations that stress softening is absent if the secondary strain axis is perpendicular to the first. The network chain density appears to be unchanged. Our mechanism conserves the number of network chains; only the entanglement density is reduced with respect to the original strain axis. Over long times or at elevated temperatures, thermal motion of the connecting chains could produce new entanglements. However, for the time spans of the experiments, we expect that removing entanglements causes changes to the network conformation that are essentially permanent, consistent with experimental observations [24]. For subsequent strains larger than the first, new entanglements may be encountered and removed in the same manner as described above, forcing the stress to recover to previous levels. This would account for the material's apparent memory of its previous maximum strain state. Clearly, whether two adjacent chains are entangled depends on their orientation with respect to the strain axis. It follows that, under tensile strain, only those entanglements associated with the strain axis are removed; entanglements associated with strains along axes perpendicular to the first strain would likely not be affected. From this observation, we can then predict that, if the material is strained along an axis orthogonal to the first strain axis, stress softening should not be observed. The experimental data shown in Fig. 2 confirms that this is indeed the case. If chains were tearing loose from the filler particles, as proposed by some earlier

theories, we would expect to see a reduction in stress for all strain directions. An interesting question is: does the removal of an entanglement associated with one strain axis lead to the creation of 'new' entanglement with respect to an orthogonal axis? The resolution of this question will have to await the next generation of tertiary strain experiments in which we will cut and strain a sample perpendicular to the secondary strain axis, that is, parallel to the initial strain. However, we note in Fig. 2 that the stress for perpendicular secondary strains appears to be about the same as the initial stress, suggesting that 'new' entanglements are not being created.

We define the energy density associated with the Mullins effect (Mullins energy) as the integrated stress of the first extension of a sample, up to some value of the strain. For a strain of 300%, the value calculated from the data in Fig. 1 is about 8.7 MPa, corresponding to an energy density of 8.7 J cm^{-3}. Our proposed mechanism for stress softening relates this energy to the product of two terms: the energy required to effect a chain crossing and their density. The chaincrossing energy is the sum of the binding energy of the attached chain plus the work done to overcome the frictional force associated with the exposed bonding sites on the particle surface. We can obtain an estimate of the average chain binding energy from previous work on silica-filled PDMS. In that study [29], atomistic simulations of a PDMS chain interacting with itself and/or a hydroxylated silica surface were used to develop an analytic model for silica-filled PDMS under tensile strain. Free parameters in the model were chosen to fit the experimental tensile stress/strain for un-crosslinked silica-filled PDMS [28]. The average binding energy between the PDMS chains and the silica particles that is consistent with this fit is about 25 kcal/mole. Interestingly, this is close to Bueche's estimate [12] for the binding energy between carbon black particles and styrene-butadiene polymers of 22 kcal/mol. For an estimate of the frictional work, we use the same value, arguing that the displacing (sliding) chain should traverse, and temporally bind to all of the binding sites originally covered by the attached chain. Our estimate of the total average energy to remove a chain entanglement is then about 50 kcal/mol. Dividing the Mullins energy density by this value yields a chain entanglement density of 2.5×10^{19} cm^{-3} for a strain of 300%. This corresponds to a molecular weight between entanglements of ~20,000 Da. This value is comparable to the range of published [31] values of the chain entanglement spacing (deduced from viscosity experiments) of 8000–12,000 Da. Our results then suggest that the removal of only about one half of the chain entanglements can account for the observed Mullins energy. However, the term 'entanglement' is not well defined and we cannot claim the relative chain conformations to which we apply the term is the same phenomenon operative in the viscosity experiments, but it is not unreasonable.

The shape of our stress vs. strain curves for the initial extension, which is typical of other experimental results [26,32–34] in the literature, exhibits a steep increase in stress, followed by a more gradual, nearly linear increase with strain up to the point of tensile failure. According to our proposed mechanism, the stress is due to the rate (with respect to strain) at which chain crossings occur. Neglecting for the moment the fact that the chains initially have slack, we conjecture that the chain-crossing rate is proportional to the angular density of chain end-to-end vectors.

$$s(\lambda) = \alpha H(\lambda), \tag{1}$$

where s is the stress, λ is the extension factor (one plus the experimental strain), α is a proportionality constant and H is the angular density of chains. As the network chains become more aligned with the strain axis, the density of chain crossing events increases, leading to an increase in stress. We may obtain an estimate for H starting with the usual assumption that tensile strain can be described by an affine transformation. Consider a chain connecting two network nodes, one at the origin, the other at z and ρ, (axial and radial coordinates) in cylindrical geometry that is strained along the z-axis. The node coordinates transform according to

$$z' = \lambda z, \quad \rho' = \sqrt{\lambda}\rho, \tag{2}$$

Using the Pythagorean theorem, we obtain an expression for the initial angle between the chain end-to-end vector and the strain axis given by

$$\theta = \cos^{-1}\left(\frac{z}{(\rho^2 + z^2)^{1/2}}\right). \tag{3}$$

For an affine transformation, the distance between two nodes scales as

$$\frac{r_\lambda}{r_0} = \left[\frac{\sin^2\theta}{\lambda} + \lambda^2\cos^2\theta\right]^{1/2} \tag{4}$$

where r_0 and r_λ are the original and transformed node separation distances, respectively. The chain end-to-end angle with respect to the strain axis transforms as

$$\theta_\lambda = \cos^{-1}\left(\frac{\lambda\cos\theta}{r_\lambda/r_0}\right). \tag{5}$$

We obtain the average chain end-to-end angle as a function of extension by integrating over all possible original angles.

$$\theta_{\text{avg}} = \frac{2}{\pi}\int_0^{\pi/2}\theta_\lambda \mathrm{d}\theta \tag{6}$$

A plot of Eq. (6) is shown in Fig. 5. For an estimate of the angular density of chain end-to-end vectors, we will use the inverse of the average angle given by

$$H(\lambda) = \theta_{\text{avg}}^{-1} = \left[\frac{2}{\pi}\int_0^{\pi/2}\cos^{-1}\left(\frac{\lambda\cos\theta}{\left[\frac{\sin^2\theta}{\lambda} + \lambda^2\cos^2\theta\right]^{1/2}}\right)\mathrm{d}\theta\right]^{-1} \tag{7}$$

Eq. (7) was evaluated numerically and a plot with α set to 2.42 is shown in Fig. 6 compared to the experimental stress/strain data for the first extension. Both have straight lines included for comparison. The arbitrary factor of 2.42 was chosen to yield

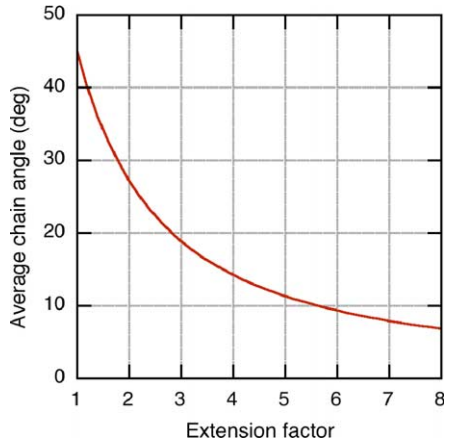

Fig. 5. Average network chain end-to-end angle as a function of extension factor. For large extensions, network chains progressively align with strain axis.

the same slope as the experimental data. Above the low strain region, we see that the shape of the average angular chain density function is qualitatively the same as the experimental stress, i.e. slightly concave. However, there is some disagreement with experiment—not surprising in view of the simplicity of our model. The model has a finite value at zero extension (the experimental stress does not), and the model curve is displaced horizontally from the experimental stress. We believe that these discrepancies can be attributed to the fact that we have ignored slack in the network chains, treating them simply as rigid end-to-end vectors. Obviously, chain slack must be removed (in response to the applied strain) before a chain-crossing event can occur, i.e. the chain must be taut. If we assume that all chains initially have slack in an amount proportional to their end-to-end distance, then we may express the chain lengths as

$$L = (1 + b)r_0, \tag{8}$$

where L is the chain length, b is a constant and r_0 is the initial node separation distance. We see that chains initially aligned close to the strain axis will not become taut until the extension approaches $1+b$, that is, we must replace λ by $\lambda+b$ in $H(\lambda)$. If we make this adjustment to Eq. (1) and set b equal to 1.14, the model is then consistent with experiment. However, this result is true only for chains initially aligned close to the strain axis; chains aligned at finite angles with respect to the strain axis will become taut at higher strains. The assumption contained in Eq. (8) also ignores the important fact that the ratio of chain lengths to node separation distances is actually a distribution. All that we can claim from this is that, if we were able to include chain slack in our formalism, it would tend to move the model closer to experiment and that the amount of slack required to do so is not unreasonable.

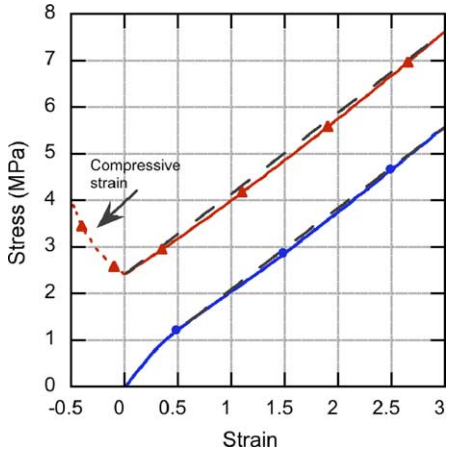

Fig. 6. Comparison of angular density of chains function, $H(\lambda)$ (triangles), and experimental data (circles). The experimental data is for the initial tensile strain and the angular density function has been scaled to have the same slope as the experimental data. Also shown adjacent to each curve is a straight line (dashed) for comparison. $H(\lambda)$ for compressive strains $\lambda<0$) is also shown.

Eq. (7) is also valid for extensions less than one, i.e. compressive strains, with the proviso that the average chain angle is now defined as the complement of θ_{avg}, since the chains align normal to the strain axis. A prediction for this type of strain is shown in Fig. 6 by the dotted line. We show the compressive stress as having the same sign as tensile stress for plotting convenience; by convention, it is usually considered to be negative. For the same reasons given above, once a chain crossing occurs, it will not be re-established as the material returns to its original shape. Consequently, stress softening should be observed during the second and subsequent compressions. We are not aware of any experimental results in silica-filled PDMS to which these results may be compared, however, it has been observed in carbon black filled natural rubber [33].

5. Conclusions

Our experimental results show that stress softening does not occur in silica-filled PDMS under tensile strain if the second strain axis is orthogonal to the original strain axis. This result provides valuable insight into the origin of the Mullins effect. We have identified a physical mechanism that accounts for the initial stress softening (the Mullins effect), namely that the tensile stress on the first extension is due to chain entanglements being removed by one chain sliding under another chain at its attachment point to a filler particle. The mechanism that we have described is consistent with a number of experimental observations including some of the distinguishing characteristics of the Mullins effect: (1) the published chain entanglement spacing, (2) the shape of the initial stress/strain curve, (3) the apparent material memory of the previous maximum strain, (4) no stress softening if the secondary strain is transverse to the first, (5) the stress softening is essentially permanent. Our model also predicts that stress softening should occur for compressive strains and provides an estimate for the modulus. If the interfacial bonding energy between the polymer and the filler particle surface can be determined independently, this theory will provide a valuable means for determining the entanglement spacing. The principal deficiency with this theory is that it is not yet able to realistically treat the effects of chain slack.

Acknowledgements

We wish to thank Dr Richard Browning for many helpful discussions and Richard Lesar and Lawrence Pratt for their valuable suggestions for improving the manuscript. This work was performed under the auspices of US Department of Energy, Contract No. W-7405-ENG-36.

References

[1] Bueche F. J Appl Polym Sci 1960;15:271–81.
[2] Mullins L. Rubber Chem Technol 1969;42:339–61.
[3] Speich JE, Borgsmiller L, Call C, Mohr R, Ratz PH. Am J Physiol-Cell Physiol 2005;289(1):C12.
[4] Harwood JAC, Payne AR. J Appl Polym Sci 1967;11(10):1825.
[5] Clement F, Bokobza L, Monnerie L. Rubber Chem Technol 2001;74(5): 847–70.
[6] Mark M, Ngai K, Graessley W, Mandelkesn L, Samulski E, Koenig J, et al. Physical properties of polymers. Washington, DC: American Chemical Society; 1984.
[7] Holt WL. Ind Eng Chem 1931;23(12):1471–5.
[8] Gurney HP, Tavener CH. J Ind Eng Chem 1922;14(2):134–9.
[9] Alexandrov AP, Lazurhin JS. Doklady Acad Nauk SSSR 1944;45:291.
[10] Mullins L. Rubber Chem Technol 1957;30:555–71.
[11] Mullins L. Rubber Chem Technol 1948;21:281–300.
[12] Bueche F. Rubber Chem Technol 1960;10:107–14.
[13] Govindjee S, Simo JC. J Mech Phys Solids 1991;39(1):87–112.
[14] Govindjee S, Simo JC. Int J Solids Struct 1992;29(14/15):1737–51.
[15] Marckmann G, Verron E, Gornet L, Chagnon G, Charrier P, Fort P. J Mech Phys Solids 2002;50(9):2011–28.
[16] Ogden RW, Roxburgh DG. In: Dorfmann A, Muhr A, Balkema AA, editors. An energy-based model of the Mullins effect. First European conference on constitutive models for rubber, 1999. p. 23–8.
[17] Ogden RW, Roxburgh DG. Proc R Soc London, Ser A-Math Phys Eng Sci 1999;455(1988):2861–77.
[18] Kluppel M. Macromol Symp 2003;200:31.
[19] Qi HJ, Boyce MC. J Mech Phys Solids 2004;52(10):2187.
[20] Zhong A. Int J Solids Struct 2005;42(13):3967.
[21] Dorfmann A. Int J Solids Struct 2005;42(16/17):4909.
[22] Horgan CO, Ogden RW, Saccomandi G. Proc R Soc London, Ser A-Math Phys Eng Sci 2004;460(2046):1737.
[23] Gent AN. Rubber Chem Technol 1996;69(1):59.
[24] Hawley ME, Wrobleski DA, Orler EB, Houlton R, Chitanvis KE, Brown GW, et al. Materials research society symposium—proceedings SO—mechanical properties of nanostructured materials and nanocomposites. vol. 791 2003 p. 93–98 [symposium on mechanical properties of nanostructured materials and nanocomposites held at the 2003 MRS Fall meeting mechanical properties of nanostructured materials and nanocomposites, Boston, MA., US, vol. 791; 2003. p. 93–8].
[25] Boonstra BB. Polymer 1979;20(6):691–704.
[26] Kilian HG, Strauss M, Hamm W. Rubber Chem Technol 1994;67(1): 1–16.
[27] Tsige M, Soddemann T, Rempe SB, Grest GS, Kress JD, Robbins MO, et al. J Chem Phys 2003;118(11):5132.
[28] Boonstra BB, Cochrane H, Dannenberg EM. Rubber Chem Technol 1975; 48:558.
[29] Hanson DE. J Chem Phys 2000;113(17):7656–62.
[30] Lapra A, Clement E, Bokobza L, Monnerie L. Rubber Chem Technol 2003;76(1):60–81.
[31] Ferry JD. Viscoelastic properties of polymers. New York: Wiley; 1980.
[32] Clement F, Lapra A, Bokobza L, Monnerie L, Menez P. Polymer 2001; 42(14):6259–70.
[33] Mars WV, Fatemi A. J Eng Mater Technol, Trans ASME 2004;126(1): 19–28.
[34] Bokobza L, Rapoport O. J Appl Polym Sci 2002;85(11):2301–16.